Calculation of Projected Bond-Orientational Order Parameters to Quantify Local Symmetries from Transmission Diffraction Data

A. C. Y. Liu,[1,2] R. F. Tabor,[3] L. Bourgeois,[1,4] M. D. de Jonge,[5] S. T. Mudie,[5] and T. C. Petersen[2]
[1]*Monash Centre for Electron Microscopy, Monash University, Clayton, 3800 Victoria, Australia*
[2]*School of Physics and Astronomy, Monash University, Clayton, 3800 Victoria, Australia*
[3]*School of Chemistry, Monash University, Clayton, 3800 Victoria, Australia*
[4]*Department of Materials Science and Engineering, Monash University, Clayton, 3800 Victoria, Australia*
[5]*Australian Synchrotron, Clayton, 3168 Victoria, Australia*
(Received 15 December 2015; published 18 May 2016; corrected 3 June 2016)

The bond-orientational order parameters introduced by Steinhardt *et al.* [Phys. Rev. B **28**, 784 (1983)] have been an invaluable measurement tool for assessing short-range order in disordered, close-packed assemblies of particles in which the particle positions are known. In many glassy systems the measurement of particle position is not possible or limited (field of view, thickness, resolution) and the bond-orientational order parameters cannot be measured, or adequately sampled. Here we calculate a set of rotationally averaged, projected bond-orientational order parameters that reflect the symmetries of close-packed particle clusters when projected onto a plane. We show by simulation that these parameters are unique fingerprints that can be directly compared to angular correlations in limited-volume, transmission geometry, diffraction patterns from close-packed glassy assemblies.

DOI: 10.1103/PhysRevLett.116.205501

The role of local structures in glass formation and properties is a long-standing subject that is still contested in contemporary debate [1]. In close-packed systems, it has long been thought that the stability of icosahedral clusters over nearest-neighbor length scales in the liquid [2] contributes greatly to the slowing structural dynamics at the glass transition. More recent work has suggested that any "locally favoured structure" can slow dynamics [3], with icosahedra still potentially playing a role in preventing crystallization [4]. Other contrasting studies identify the extent of ordering in the liquid next to a crystal interface as more critical to glass formability than any local structure in the bulk [5]. Despite the lack of consensus regarding the role of local structure, the concept of the three-dimensional bond-orientational order parameters and related invariant quantities introduced by Steinhardt, Nelson, and Ronchetti [6] has been extremely powerful in canvassing order in amorphous close-packed systems with known particle positions. Using these concepts, computer-generated models and confocal microscopy data sets can be distinguished by their dominant short-range order characteristics and also the spatial variation of these local preferred structures [3,4,6].

While there have been many developments in the implementation of scanning transmission confocal electron microscopy [7–9], measurement of atomic coordinates in three dimensions in disordered materials has not been achieved. Confocal optical microscopy has limits to field of view and depth, which are an impediment to obtaining statistical information about order in bulk materials. In contrast, scanning transmission diffraction experiments can statistically sample many structural configurations. Limited-volume diffraction measurements of disordered systems in a transmission geometry display variations in diffracted intensity that reflect local order (Fig. 1) [10–13]. The collimated and coherent illumination can be limited laterally by an aperture upstream of the specimen. The beam can be scanned (scanning transmission electron microscope) or the stage can be translated (scanning transmission x-ray diffraction) to collect an ensemble of diffraction patterns.

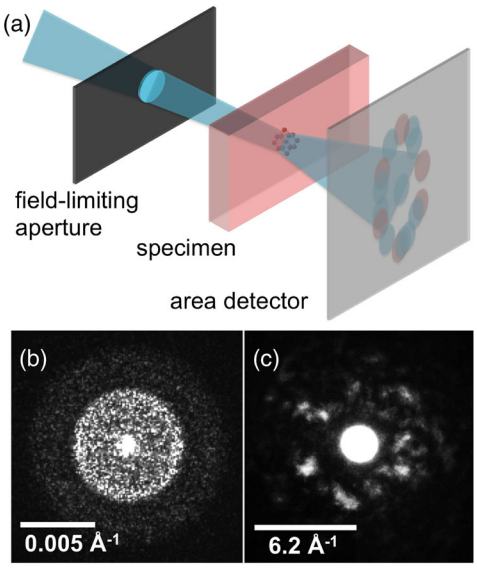

FIG. 1. (a) Schematic of limited-volume diffraction measurements of disordered materials. An upstream aperture in either the near or far fields limits the illumination area, resulting in the diffraction pattern of the aperture modulated by the diffracted intensity from the disordered structure. (b) X-ray microdiffraction pattern of a 300 nm diameter colloidal glass with a 20 μm near-field aperture. (c) Electron nanodiffraction pattern of a $Zr_{36}Cu_{64}$ glass with a 5 μm aperture in the far field and 5.6 Å probe size.

Scanning x-ray microdiffraction and scanning electron nanodiffraction have been applied to colloidal [10,14] and atomic systems [11,15], respectively. Much progress has been made in interpreting the fluctuations and angular correlations in the diffracted intensity employing simulation [11,15] and by employing reverse Monte Carlo calculations to refine models [16,17]. Modeling diffraction from disordered materials is computationally intensive, and, in general, a number of simplifying assumptions such as kinematical diffraction are employed to reduce calculation size. Moreover, despite the inclusion of multiple experimental constraints, models produced by reverse Monte Carlo calculation may not be unique. More direct techniques to probe order from such measurements are sought.

In this Letter, we calculate the rotationally averaged Fourier coefficients of projected angular symmetries in kinematical diffraction patterns from archetypal nearest-neighbor clusters. These calculations show that these rotationally averaged Fourier coefficients are a unique fingerprint of the short-range cluster in the projection geometry, analogous to the invariant bond-orientational order parameters in three dimensions. We demonstrate by simulation that these rotationally averaged Fourier coefficients are a comparable quantity to the magnitudes of angular correlations extracted from limited-volume diffraction patterns from glasses [18]. Thus, these unique fingerprints of the projected angular symmetry of nearest-neighbor clusters have the potential to be used to measure the proportions of locally preferred structures directly from experiment and become a powerful tool in understanding the role of structure in glass-forming systems.

The symmetries present in limited-volume diffraction patterns from disordered materials are often subtle. To detect and quantify the symmetries present in each pattern obtained at position $\vec{r} = (x, y)$ in the lateral plane of the specimen, the angular autocorrelation function as a function of scattering vector magnitude has been employed [Eq. 1] [11,14,15]. The scattering vector magnitude is $|\vec{q}| = q = \sqrt{q_x^2 + q_y^2} = 4\pi \sin\theta/\lambda$, with λ as the wavelength.

$$C(\vec{r}, q, \Delta) = \frac{\langle I(q,\phi)I(q,\phi+\Delta)\rangle_\phi - \langle I(q,\phi)\rangle_\phi^2}{\langle I(q,\phi)\rangle_\phi^2}. \quad (1)$$

Here, $I(\vec{r}, q, \phi) = I(q, \phi)$ is the intensity diffracted into a given q and azimuthal angle ϕ, and $\langle\rangle_\phi$ denotes averaging over the azimuthal angle at a given q [19], $\langle X\rangle_\phi = (1/2\pi)\int_0^{2\pi} X d\phi$. These angular autocorrelation functions are decomposed into a Fourier series to extract the magnitudes of each symmetry at each scattering vector,

$$C(\vec{r}, q, \Delta) = \sum_{n=-\infty}^{n=\infty} C_q^n e^{in\Delta}, \quad (2)$$

where the Fourier coefficients are

$$C_q^n = \frac{1}{2\pi}\int_0^{2\pi} C(\vec{r}, q, \Delta) e^{-in\Delta} d\Delta, \quad (3)$$

$$C_q^n = \frac{1}{2\pi}\int_0^{2\pi} \frac{\int_0^{2\pi}\frac{1}{2\pi} I(q,\phi)I(q,\phi+\Delta)d\phi - \frac{1}{4\pi^2}[\int_0^{2\pi} I(q,\phi)d\phi]^2}{\frac{1}{4\pi^2}[\int_0^{2\pi} I(q,\phi)d\phi]^2} e^{-in\Delta} d\Delta$$

$$= \frac{1}{I_q^0 . I_q^0}\frac{1}{4\pi^2}\int_0^{2\pi} I(q,\phi)e^{in\phi}d\phi \int_0^{2\pi} I(q,\Delta)e^{-in\Delta}d\Delta - \frac{1}{2\pi}\int_0^{2\pi} e^{-in\Delta}d\Delta = \begin{cases} \frac{I_q^n . I_q^n}{I_q^0 . I_q^0} = \frac{c_q^n}{c_q^0} & \text{if } n \neq 0 \\ 0 & \text{if } n = 0. \end{cases} \quad (4)$$

This result shows that the Fourier coefficients of the autocorrelation c_q^n are a function of the Fourier coefficients of the intensity I_q^n [19].

For materials in which the reciprocal specimen thickness is comparable to the Ewald sphere curvature and in which multiple diffraction events can occur, the diffraction pattern will not possess Friedel symmetry and the angular autocorrelation function will display odd symmetries [18]. Thickness can be limited to the extent that the Ewald sphere can be approximated as flat (20 μm for 5 keV x rays and 4 nm for 300 keV electrons), but multiple scattering is still present for these low thicknesses. Recently, a technique to correct the average angular symmetry magnitudes from an ensemble of dynamical diffraction patterns and recover the average kinematical symmetry magnitudes was demonstrated [18]. Here, we derive the rotationally averaged magnitudes of these Fourier coefficients for close-packed atomic clusters using the simplifying assumptions of planar Ewald sphere and kinematical diffraction. This derivation is similar to that presented by Altarelli, but with many simplifying assumptions and restrictions that can be applied to present experimental geometries and analysis [11,18].

In the limit of a flat Ewald sphere and for N scatterers with isotropic form factors, $f(\vec{q}) = f(q)$, the diffracted intensity equals

$$I(\vec{q}) = \lambda^2 \sum_i^N \sum_j^N f_i(q) f_j(q) e^{i\vec{q}\cdot\vec{r}_{ij}}. \quad (5)$$

$\vec{r}_{ij} = \vec{r}_i - \vec{r}_j$ is the distance between scatterers. We can simplify this expression:

$$I(\vec{q}) \approx \lambda^2 f^2(q) \sum_i^N \sum_j^N e^{iqr_{ij}\cos(\phi-\phi_{ij})}$$

$$= \lambda^2 f^2(q) \sum_i^N \sum_j^N \sum_{m=-\infty}^{m=+\infty} i^m J_m(qr_{ij}) e^{im(\phi-\phi_{ij})}. \quad (6)$$

Here ϕ and ϕ_{ij} are the azimuthal angles of $\vec{q}$ and $\vec{r}_{ij}$, and in the final line we have employed the Jacobi-Anger expression:

$$e^{iz\cos\theta} = \sum_{m=-\infty}^{m=+\infty} i^m J_m(z) e^{im\theta}. \tag{7}$$

We can now evaluate the Fourier coefficients of the diffracted intensity and so calculate the Fourier coefficients of the angular autocorrelation:

$$\begin{aligned} I_q^n &= \lambda^2 f^2(q) \sum_i^N \sum_j^N \sum_{m=-\infty}^{m=+\infty} i^m J_m(qr_{ij}) \\ &\quad \times e^{-im\phi_{ij}} \frac{1}{2\pi} \int_0^{2\pi} e^{i(m-n)} d\phi \\ &= \lambda^2 f^2(q) \sum_i^N \sum_j^N \sum_{m=-\infty}^{m=+\infty} i^m J_m(qr_{ij}) e^{-im\phi_{ij}} \delta_{mn} \\ &= \lambda^2 f^2(q) \sum_i^N \sum_j^N i^n J_n(qr_{ij}) e^{-in\phi_{ij}}. \end{aligned} \tag{8}$$

The Fourier coefficients of the normalized angular autocorrelation are thus

$$c_q^n / c_q^0 = \left| \frac{\sum_i^N \sum_j^N i^n J_n(qr_{ij}) e^{-in\phi_{ij}}}{\sum_k^N \sum_l^N J_0(qr_{kl})} \right|^2. \tag{9}$$

We calculated the Fourier coefficients of the angular autocorrelation functions from kinematical diffraction patterns of unit clusters. The 13-atom icosahedral cluster (icos) oriented down the tenfold axis of symmetry displays only a strong tenfold symmetry as anticipated [Fig. 2(a)]. A symmetric cluster such as an icosahedron oriented down an arbitrary orientation displays many symmetries [Fig. 2(b)]. Averaging a face-centred cubic (fcc) cluster over 1000 random orientations, we see that the magnitude of the Fourier coefficients is appreciable only in a range of scattering vector close to $1.23 \times 2\pi/d = 7.7$ Å^{-1}, as predicted by the Ehrenfest relation [20]. We averaged the magnitudes of the Fourier coefficients from the fcc cluster over 20 000–160 000 random rotations in the scattering vector range of 5.5–11 Å^{-1} that corresponds to the first main diffraction peak. Both the unnormalized and normalized averaged Fourier coefficients converge quickly to stable values [21]. These values provide a unique fingerprint of the projected symmetries of the fcc cluster.

The average magnitudes of the Fourier coefficients from 160 000 random orientations for the fcc, icos, 13-atom hexagonal close-packed (hcp), 9-atom body-centred cubic (bcc), and 8-atom simple cubic (sc) clusters are displayed in Fig. 3. It is clear that each cluster has a unique pattern of average projected symmetry magnitudes. For example, the sc cluster has only predominantly low-order symmetries compared to the other clusters. The unnormalized Fourier coefficients and the normalized Fourier coefficients are not equivalent, with the normalized Fourier coefficients

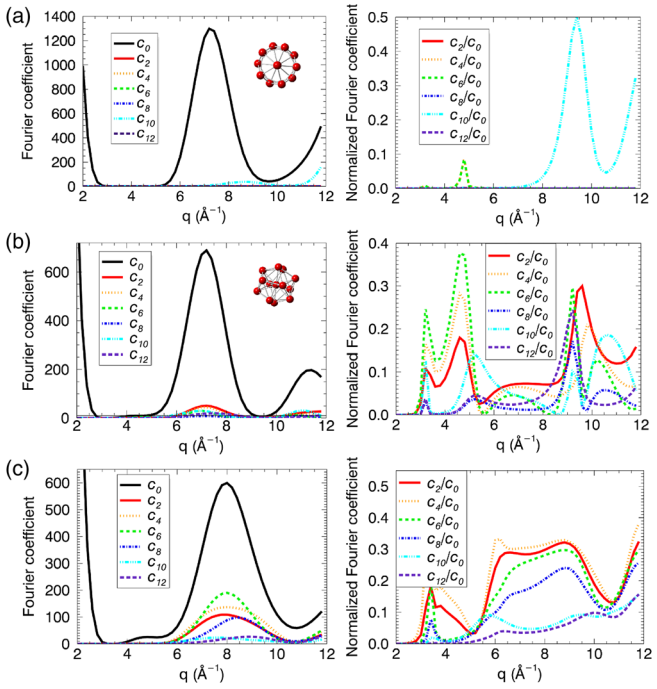

FIG. 2. Unnormalized and normalized Fourier coefficients of (a) the icos cluster oriented down its tenfold symmetry axis, (b) the icos cluster oriented in an arbitrary rotation, and (c) the fcc cluster averaged over 1000 random rotations.

providing clearer trends. The fcc, bcc, and sc clusters have the greatest magnitude in the fourfold symmetry. The hcp and icos clusters have the greatest magnitude in the sixfold symmetry. In Fig. 3(c) we display the magnitude of the

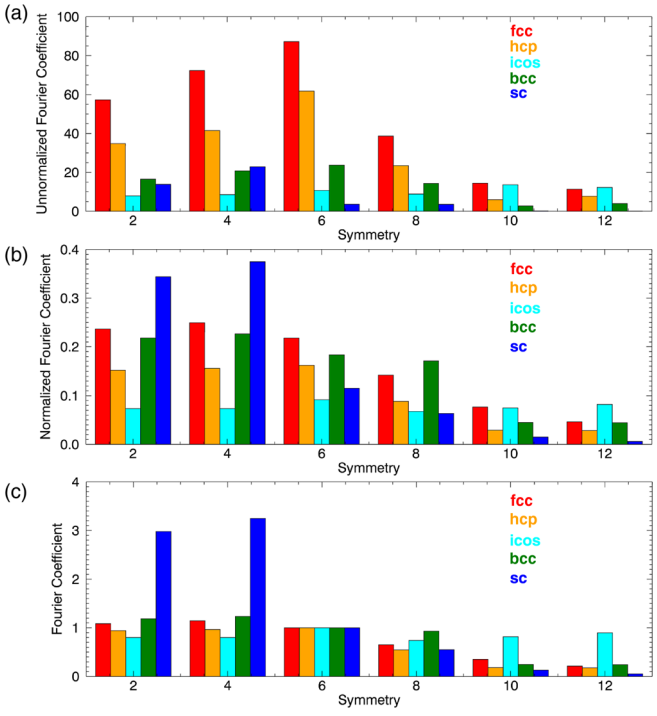

FIG. 3. Unnormalized (a), normalized (b), and normalized to sixfold (c) Fourier coefficients of the fcc, hcp, icos, bcc, and sc clusters averaged over 160 000 random orientations.

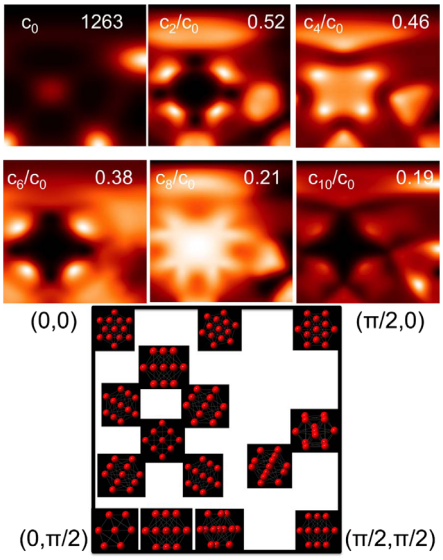

FIG. 4. Top: Maps of Fourier coefficients from the fcc cluster calculated with rotation angles around the x and y axes in the range of $(0, \pi/2)$. The maximum intensity is displayed in each map. Bottom: Schematic showing the cluster orientations at the map poles.

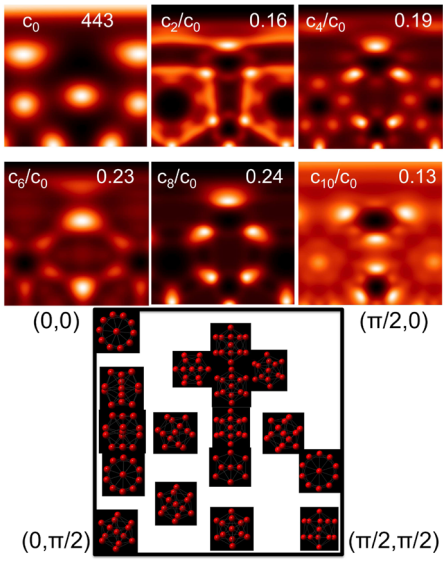

FIG. 5. Top: Maps of Fourier coefficients from the icos cluster calculated with rotation angles around the x and y axes in the range of $(0, \pi/2)$. The maximum intensity is displayed in each map. Bottom: Schematic showing the cluster orientations at the map poles.

normalized symmetry magnitudes relative to the sixfold Fourier coefficient. This exaggerates the previously noted trends and provides a means to internally normalize these symmetry magnitudes.

The icos cluster shows the most even distribution and lowest values overall of normalized symmetry magnitudes, indicating that this cluster has lower projected symmetry than the other ones. This is not intuitive as the icos cluster in three dimensions (I_h point group) has a much higher point group symmetry (60) than, for example, the point group of the fcc cluster (O_h) with point symmetry of 24 [21]. Projection of a structure diminishes the symmetry of the object. Even so, the higher symmetry of the icos cluster includes 60 rotational axes and 15 mirror planes that will still give rise to many projected symmetries. To understand this result, maps of Fourier coefficients were calculated using rotation angles around the x and y axes in the range $[0, \pi/2]$ (fcc, Fig. 4; icos, Fig. 5; sc, hcp, and bcc, Supplemental Material [21]). As anticipated, the maps from the icos cluster are more highly featured than the maps from the fcc cluster, but their average magnitude is lower. This is due to the fact that the projected angles between atoms (based on $2\pi/5$) do not give large values for even symmetries. The term $e^{-in\phi_{ij}}$ is low for many orientations. This symmetry degradation due to projection from three dimensions to two is analogous to the reduction in translational symmetry of quasicrystals when the spatial dimension is reduced from six to three.

The rotationally averaged Fourier coefficients are a unique fingerprint of the projected symmetries of the short-range cluster. Comparable quantities would be obtained from limited-volume diffraction patterns from a dilute gas of randomly oriented clusters. Are these characteristic symmetries also useful for dense, random, close-packed structures? To answer this, we compare the magnitudes of the Fourier coefficients for strings of structurally uncorrelated fcc clusters and the average of the magnitudes of Fourier coefficients for the same individual fcc clusters [four clusters, Fig. 6(a); two and three clusters, Supplemental Material [21]]. Differences between these quantities reflect the degree to

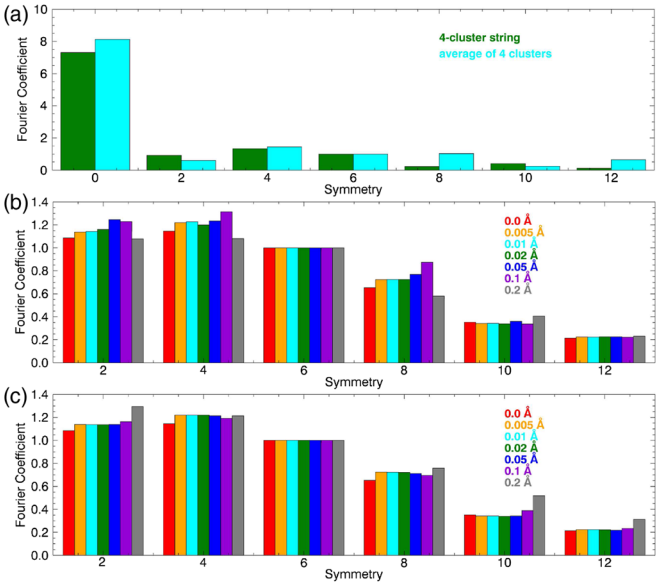

FIG. 6. (a) Comparison between the magnitudes of the Fourier coefficients for a string of four structurally uncorrelated clusters and the average of the magnitudes of Fourier coefficients for the same individual clusters. (b) Rotationally averaged Fourier coefficients for a fcc cluster with a single systematic distortion. (c) Averaged Fourier coefficients for 160 000 fcc clusters with random orientations and random distortions. All Fourier coefficients are normalized to the sixfold coefficient.

which correlations between particles in different clusters (viewed in projection) contribute to the Fourier coefficients. Note that this is the worst scenario in which neighboring clusters have no structural correlation. In a three-dimensional close-packed glass correlations can extend over many clusters. With increasing cluster number there is growing disagreement between the symmetry magnitudes from the string of clusters and the averaged magnitudes from the individual clusters. Despite this, general trends are retained. This demonstrates that the rotationally averaged Fourier coefficients from archetypal short-range clusters can be compared to limited-volume diffraction patterns from dense three-dimensional glasses for limited thicknesses, an experimentally accessible regime [11,18].

Realistic, random, close-packed systems contain a degree of polydispersity (colloids) or bond length variation due to chemical ordering (multicomponent metallic glasses) resulting in distorted clusters. These distortions might be systematic, or distributed among many configurations. We recalculated the rotationally averaged Fourier coefficients for a fcc cluster with a systematic distortion by randomly displacing the particle positions with standard deviations of 0.005–0.2 Å (0.5%–20% distortion). As seen in Fig. 6(b) (Supplemental Material [21] for unnormalized Fourier coefficients), the average projected symmetry fingerprint is preserved for all these displacements, with marked similarity seen for displacements up to 5%, similar to variations in the first nearest-neighbor position of real systems. To model distributed distortions, we calculated the averaged Fourier coefficients for 160 000 fcc clusters with random orientations and also random particle displacements of standard deviation 0.005–0.2 Å [Fig. 6(c) and Supplemental Material [21] for unnormalized Fourier coefficients]. At the highest random displacements (0.1 and 0.2 Å) the Fourier coefficients for tenfold and twelvefold symmetry are slightly elevated, flattening the distribution. These displacements are much greater than in realistic systems, and indeed, with such high displacements, cluster transformation could occur.

We have calculated the rotationally averaged Fourier coefficients of the angular autocorrelation functions from kinematical limited-volume diffraction patterns for archetypal short-range clusters. These quantities converge to stable values giving a fingerprint of the average projected symmetries that is unique for each cluster. These unique fingerprints will be a powerful new tool to examine the existence and nature of preferred local structures in glasses. For example, a least squares fitting procedure could be used to quantify populations of clusters from the average angular symmetry magnitudes in ensembles of limited-volume diffraction patterns. Our analysis is developed for disordered, solid, close-packed systems. Similar approaches may be useful for the study of liquids [22] and suspensions of anisotropic particles and molecules.

A. C. Y. L. acknowledges the support of the Science Faculty, Monash University. T. C. P. and A. C. Y. L. acknowledge support from the Monash Centre for Electron Microscopy. The authors acknowledge use of facilities within the Monash Centre for Electron Microscopy. This research used equipment funded by Australian Research Council grant ARC Funding (LE0454166). This research was undertaken in part on the SAXS/WAXS beam line at the Australian Synchrotron, Victoria, Australia. We thank Nigel Kirby and Adrian Hawley for their assistance. Joanne Etheridge is gratefully acknowledged for many useful discussions.

[1] C. P. Royall and S. R. Williams, Phys. Rep. **560**, 1 (2015).
[2] F. C. Frank, Proc. R. Soc. A **215**, 43 (1952).
[3] C. P. Royall, S. R. Williams, T. Ohtsuka, and H. Tanaka, Nat. Mater. **7**, 556 (2008).
[4] M. Leocmach and H. Tanaka, Nat. Commun. **3**, 974 (2012).
[5] C. Tang and P. Harrowell, Nat. Mater. **12**, 507 (2012).
[6] P. J. Steinhardt, D. R. Nelson, and M. Ronchetti, Phys. Rev. B **28**, 784 (1983).
[7] P. D. Nellist, G. Behan, A. I. Kirkland, and C. J. D. Hetherington, Appl. Phys. Lett. **89**, 124105 (2006).
[8] S. P. Frigo, Z. H. Levine, and N. J. Zaluzec, Appl. Phys. Lett. **81**, 2112 (2002).
[9] C. Zheng, Y. Zhu, S. Lazar, and J. Etheridge, Phys. Rev. Lett. **112**, 166101 (2014).
[10] M. M. J. Treacy, J. M. Gibson, L. Fan, D. J. Paterson, and I. McNulty, Rep. Prog. Phys. **68**, 2899 (2005).
[11] A. C. Y. Liu, M. J. Neish, G. Stokol, G. A. Buckley, L. A. Smillie, M. D. de Jonge, R. T. Ott, M. J. Kramer, and L. Bourgeois, Phys. Rev. Lett. **110**, 205505 (2013).
[12] A. Hirata, P. Guan, T. Fujita, Y. Hirotsu, A. Inoue, A. R. Yavari, T. Sakurai, and M. Chen, Nat. Mater. **10**, 28 (2011).
[13] S. O. Hruszkewycz, T. Fujita, M. W. Chen, and T. C. Hufnagel, Scr. Mater. **58**, 303 (2008).
[14] P. Wochner, C. Gutt, T. Autenrieth, T. Demmer, V. Bugaev, A. D. Ortiz, A. Duri, F. Zontone, G. Grübel, and H. Dosch, Proc. Natl. Acad. Sci. U.S.A. **106**, 11511 (2009).
[15] J. M. Gibson, M. M. J. Treacy, T. Sun, and N. J. Zaluzec, Phys. Rev. Lett. **105**, 125504 (2010).
[16] J. Hwang, Z. H. Melgarejo, Y. E. Kalay, I. Kalay, M. J. Kramer, D. S. Stone, and P. M. Voyles, Phys. Rev. Lett. **108**, 195505 (2012).
[17] M. M. J. Treacy and K. B. Borisenko, Science **335**, 950 (2012).
[18] A. C. Y. Liu, G. R. Lumpkin, T. C. Petersen, J. Etheridge, and L. Bourgeois, Acta Crystallogr. Sect. A **71**, 473 (2015).
[19] M. Altarelli, R. P. Kurta, and I. A. Vartanyants, Phys. Rev. B **82**, 104207 (2010).
[20] A. Guinier, *X-Ray Diffraction: In Crystals, Imperfect Crystals, and Amorphous Bodies*, 2nd ed. (Dover, New York, 1994).
[21] See Supplemental Material at http://link.aps.org/supplemental/10.1103/PhysRevLett.116.205501 for Fourier coefficients of fcc cluster averaged over 20 000–160 000 random orientations, a table of the I_h and O_h point symmetries, maps of the Fourier coefficients for the sc, bcc, and hcp clusters and Fourier coefficients for distorted fcc clusters.
[22] H. Tanaka, Eur. Phys. J. E **35**, 113 (2012).